Vibrational circular dichroism as a probe of solid-state organisation of derivatives of cyclic β-amino acids: Cis - and trans -2-aminocyclobutane-1-carboxylic acid

Valérie Declerck, Ariel Pérez-mellor, Régis Guillot, David Aitken, Michel Mons, Anne Zehnacker

Vibrational Circular Dichroism as a probe of solid-state organisation of derivatives of cyclic β-amino acids: *cis*- and *trans*-2-aminocyclobutane-1-carboxylic acid

Valérie Declerck,[b] Ariel Pérez-Mellor,[a] Régis Guillot,[b] David J. Aitken,[b] Michel Mons,[c] Anne Zehnacker*[a]

Abstract: Peptide models built from *cis* and *trans* 2-aminocyclobutane-1-carboxylic acids (ACBCs) are studied in the solid phase by combining FTIR absorption spectroscopy, vibrational circular dichroism (VCD), and quantum chemical calculations using density functional theory (DFT). The studied systems are N-*tert*-butyloxycarbonyl (Boc) derivatives of 2- aminocyclobutanecarboxylic acid (ACBC) benzylamides, namely: Boc−(*cis*-ACBC)−NH−Bn and Boc−(*trans*-ACBC)−NH−Bn. These two diastereomers show very different VCD signatures and intensities, that of the *trans*-ACBC derivative being one order of magnitude larger in the region of the ν(CO) stretch. The spectral signature of the *cis*-ACBC derivative is satisfactorily reproduced by that of the monomer extracted from the solid-state geometry of related ACBC derivatives, which shows that no long-range effects are implicated for this system. In terms of hydrogen bonds, the geometry of this monomer is intermediate between the C6 and C8 structures (exhibiting a 6- or 8-membered cyclic NH···O hydrogen bond) previously evidenced in the gas phase. The benzyl group must be in an extended geometry to reproduce satisfactorily the shape of the VCD spectrum in the ν(CO) range, which qualifies VCD as a potential probe of dispersion interaction. In contrast, reproducing the IR and VCD spectrum of the *trans*-ACBC derivative requires clusters larger than four units, exhibiting strong intermolecular H-bonding patterns. A qualitative agreement is obtained for a tetramer, although the intensity enhancement is not reproduced. These results underline the sensitivity of VCD to the long-range organisation in the crystal.

Keywords: VCD, β peptide, crystal structure, IR spectroscopy

Introduction

Synthetic oligomers built by assembling particular molecular building blocks can adopt regular folding patterns, which are maintained by networks of non-covalent interactions such as hydrogen bonds, locking them into well-defined conformations. The environment and the nature of the building blocks dictate the shape of these oligomers, leading to diverse secondary structures similar to those found in Nature (such as helices turns and sheets) as well as abiotic molecular architectures. In the emerging area of foldamer science, bioinspired β-amino acids (β-AA) are of special interest due to their pronounced ability to induce regular folding patterns in oligomer sequences, including helical structures in particular. Moreover, oligomers of β-AAs, also known as β-peptides, are resistant to proteolysis which is especially interesting for potential biomedical applications.[1] In β-peptides, local hydrogen bonding interactions compete with long-distance interactions. In this context, employment of cyclic β-AA monomers which incorporate a 4- to 6-membered aliphatic ring is of special interest because the monomer can possess either a *cis* or *trans* geometry and the geometric constraints imposed by the ring induce a pronounced conformational bias.[2] [3] The 4-membered ring monomer, 2-aminocyclobutane carboxylic acid (ACBC), displays a preference for local interactions implicating a six-membered (C6) or an eight-membered (C8) cyclic NH···O hydrogen bond, depending on the *cis* or *trans* ring geometry, the physical or chemical environment, and the length of the oligomer.[4]

Several studies have been conducted in solution to assess the conformational preferences of these systems. In derivatives of the *cis* stereoisomer (*cis*-ACBC), the intra-residue six-membered ring (C6) hydrogen bond suggested for the monomer in solution seems to persist in oligomers up to the octamer.[5] [6] However, the presence of a C8 monomeric structure cannot be ruled out in the condensed phase. Derivatives of the *trans* diastereoisomer (*trans*-ACBC) display a C8 hydrogen bond in the monomer and in short oligomers (up to four residues), which is superseded by 12-helix structures, implicating a series of C12 hydrogen bonds, in longer oligomers. Fewer studies have been reported under isolated conditions. Pohl et al. reported an

[a] *Dr. Ariel Pérez-Melor, Dr. Anne Zehnacker*
Institut des Sciences Moléculaires d'Orsay (ISMO), CNRS, Univ. Paris-Sud, Université Paris-Saclay, F-91405 Orsay (France)
E-mail: anne.zehnacker-rentien@u-psud.fr

[b] *Dr. Valérie Declerck, Dr. Régis Guillot, Pr. David J. Aitken*
CP3A Organic Synthesis Group and Services Communs, ICMMO, UMR 8182, Université Paris Sud, Université Paris-Saclay, Bâtiment 420, 15 Rue Georges Clemenceau, F-91405 Orsay (France)

[c] *Dr. Michel Mons*
Laboratoire Interactions, Dynamiques et Lasers (LIDYL) Univ Paris Saclay, CEA, CNRS, F-91191 Gif Sur Yvette, (France)

elegant study of simple ACBC amide derivatives under matrix isolation conditions.[7] They provided evidence for both C6 and C8 geometries in the *cis*-ACBC monomer. Surprisingly, a fully extended structure with no hydrogen bond coexisted with the expected C8 structure for the *trans*-ACBC stereoisomer. We recently applied conformer-specific laser spectroscopy to jet-cooled ACBC benzylamides, protected by a *tert*-butyloxycarbonyl (Boc) group on the N-terminus; the benzyl group was used as the requisite UV chromophore for conformer-specific spectroscopic analysis.[8] The gas-phase results confirmed the condensed-phase findings that C6 and C8 conformers both exist for monomeric *cis*-ACBC derivatives.[8] A structure involving an outstandingly strong C8 hydrogen bond was observed in the jet-cooled monomeric *trans*-ACBC derivative.[8]

The conformational preferences observed in isolated species, whether in gas phase or in solution, may be modified in the solid state due to intermolecular hydrogen bond formation. In hexamers or octamers of *trans*-ACBC, the intramolecular C12 interaction is not perturbed in the crystal lattice and the 12-helical secondary structure is similar in solution and in the solid state.[9] For shorter oligomers, however, it is expected that the intramolecular hydrogen bonds are disrupted by the formation of intermolecular hydrogen bond networks, as observed in *cis*-ACBC.[10]

Vibrational circular dichroism (VCD) has proved to be a powerful tool for the study of secondary structures in peptides and proteins.[11 12 12d, 13 14] The Amide I and II regions are especially informative as the coupling between modes localised on CO or NH of different residues has a strong signature in VCD.[15] In contrast with electronic circular dichroism (ECD) signatures, which has been used for structural characterization of helices or strands,[2, 16] VCD has not been applied yet to ACBC-based peptides, in particular to their solid state. VCD spectra of solid-state or supramolecular systems,[17] for example nanofibrils,[18] polymorphic crystals,[19] or foldamers[20] are scarce. One of the questions raised by the interpretation of VCD spectra in the solid state is the nature of the minimum size cell that is necessary for describing the system. The unit can be thought of as a monomer, like in solution.[21] In other cases, one has to take into account the crystal unit cell itself or a cluster of definite size like a dimer or a tetramer.[15c 22] Still, the intensity enhancement observed in the solid state has to be fully understood.[18, 23 24]

We present here a comparative FTIR and VCD study of the solid-state *cis*- and *trans*-ACBC derivatives, Boc−(*cis*-ACBC)−NH−Bn and Boc−(*trans*-ACBC)−NH−Bn, shown in Figure 1. These ACBC derivatives are protected by a tert-butyloxycarbonyl (Boc) group on the N-terminus and bear a benzyl amide (Bn) group on the C terminus. In what follows, Boc−(*cis*-ACBC)−NH−Bn and Boc−(*trans*-ACBC)−NH−Bn will be referred to as *cis*-ACBC and *trans*-ACBC, respectively, like in our previous publication.[8] We will focus on the vibrational spectroscopy in the amide I and II region (ν(CO) stretch and β(NH) bend region), which is very sensitive to hydrogen bond formation. The calculation strategy rests on the definition of clusters of finite size built from known X-ray structures. The IR absorption and VCD spectra are calculated for increasing sizes of the clusters until the calculations satisfactorily reproduce the experimental results, which allows determining the smallest cluster size that is necessary for reproducing the VCD spectrum of the crystal.

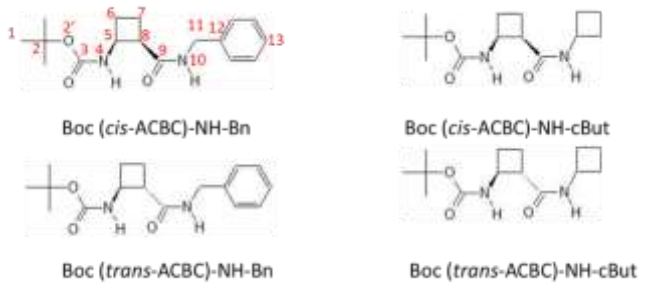

FIGURE 1 Molecules under study and numbering of atoms. ϕ = $C^3–N^4–C^5–C^8$ θ = $N^4–C^5–C^8–C^9$ ψ = $C^5–C^8–C^9–N^{10}$ ψ_{Ph}= $C^9–N^{10}–C^{11}–C^{12}$

Materials and Methods

SYNTHESIS AND CHARACTERIZATION

Compounds (−)-Boc−(*t*-ACBC)−OH, and (−)-Boc−(*c*-ACBC)−OH were prepared according to literature procedures.[25] All reagents and solvents were of commercial grade and were used without further purification. Dichloromethane was dried over activated alumina. Flash chromatography was performed with SDS silica gel (35-70 μm). Analytical thin-layer chromatography (TLC) was performed with 0.25 mm commercial silica gel plates (EMD, Silica Gel $60F_{254}$). TLC plates were visualised by UV fluorescence at 254 nm then revealed using a phosphomolybdic acid solution (10% in EtOH). Retention factors (R_f) are given for such analyses. Fourier-transform Infrared (IR) spectra were recorded in the ATR mode by deposition of the neat compound on the ATR diamond accessory. Maximum absorbance (ν) is given for significant bands in cm^{-1}. Melting points were obtained in open capillary tubes and are uncorrected. Optical rotations were measured using a 10 cm quartz cell. Values for $[\alpha]_D^T$ were obtained with the D-line of sodium at the indicated temperature *T*, using solutions of concentration (*c*) in units of g·100 mL^{-1}. Routine nuclear magnetic resonance (NMR) data were acquired on a spectrometer operating at 360 MHz for ^1H and at 90 MHz for ^{13}C. Chemical shifts (δ) are reported in ppm from tetramethylsilane. Splitting patterns for ^1H NMR signals are designated as s (singlet), d (doublet), t (triplet), bs (broad singlet) or m (multiplet). Coupling constants (^nJ) are reported in Hz. High-resolution mass spectrometry (HRMS) data were recorded using the electrospray ionization technique in positive mode (ESI+) with a tandem Q-TOF analyzer.

General Procedure for the Preparation of Benzylamides

To an ice-cold solution of Boc-amino acid (43.1 mg, 0.20 mmol, 1 eq.) in dry CH_2Cl_2 (10 mL) were added 1-hydroxybenzotriazole monohydrate (37.8 mg, 0.28 mmol, 1.4 eq.) and benzylamine (24 μL, 0.22 mmol, 1.1 eq.). The mixture was stirred for 10 min at 0 °C then 1-(3-dimethylaminopropyl)-3-ethyl carbodiimide hydrochloride (57.5 mg, 0.30 mmol, 1.5 eq.) was added. The resulting mixture was then stirred for 48 h at room temperature, then washed successively with 1 M aqueous $KHSO_4$ (5 mL) and saturated $NaHCO_3$ (5 mL). The organic layer was dried over $MgSO_4$, filtered and evaporated under reduced pressure. Flash chromatography (CH_2Cl_2/EtOAc) gave the benzyl amide.

N-Benzyl-(1R,2R)-2-(t-butyloxycarbonylamino)cyclobutane carboxamide (Boc−(t-ACBC)−NH−Bn): Coupling of (−)-Boc−(*t*-ACBC)−OH according to the general procedure, followed by flash chromatography (CH_2Cl_2/EtOAc = 80/20) gave the benzyl amide (−)-Boc−(*t*-ACBC)−NH−Bn (47.2 mg, 78%) as a white

solid. Mp 176-177 °C; R_f 0.28 (CH_2Cl_2/EtOAc = 80/20); $[\alpha]_D^{24}$ −26 (*c* 0.50, $CHCl_3$); IR (ATR) v 3336, 3299, 1681, 1644, 1531; ^{1}H NMR (360 MHz, $CDCl_3$) δ 1.39 (s, 9H), 1.75 (pseudo quint, 1H, ^2J = ^3J = 9.9 Hz), 1.86-1.99 (m, 1H), 2.02-2.23 (m, 2H), 2.86-2.98 (m, 1H), 4.08-4.20 (m, 1H), 4.35 (dd, 1H, ^2J = 14.8 Hz, ^3J = 5.0 Hz, A*B*X), 4.54 (dd, 1H, ^2J = 14.8 Hz, ^3J = 6.3 Hz, *A*BX), 5.14 (bd, 1H, ^3J = 6.3 Hz), 7.17-7.37 (m, 5H), 8.38 (bs, 1H, AB*X*); ^{13}C NMR (90 MHz, $CDCl_3$) δ 18.7, 24.9, 28.4, 43.3, 48.8, 50.1, 80.4, 127.1, 127.8, 128.5, 138.8, 156.3, 173.0; HRMS (ESI+) Calcd for $C_{17}H_{24}N_2NaO_3$ $[M + Na]^+$: 327.1679, found 327.1667.

N-Benzyl-(1R,2S)-2-(t-butyloxycarbonylamino)cyclobutanecarboxamide (Boc−(c-ACBC)−NH−Bn): Coupling of (−)-Boc−(*c*-ACBC)−OH according to the general procedure, followed by flash chromatography (CH_2Cl_2/EtOAc = 90/10) gave the benzylamide (−)-Boc−(*c*-ACBC)−NH−Bn (59.3 mg, 97%) as a white solid. Mp 162-163 °C (dec.); R_f 0.49 (CH_2Cl_2/EtOAc = 80/20); $[\alpha]_l^{24}$ −89 (*c* 0.50, $CHCl_3$); IR (ATR) v 3363, 3349, 1679, 1648, 1535, 1512; ^{1}H NMR (360 MHz, $CDCl_3$) δ 1.39 (s, 9H), 1.82-1.95 (m, 1H), 2.02-2.14 (m, 1H), 2.20-2.38 (m, 2H), 3.16-3.27 (m, 1H), 4.33-4.44 (m, 1H), 4.38 (dd, 1H, ^2J = 14.8 Hz, ^3J = 5.5 Hz, A*B*X), 4.46 (dd, 1H, ^2J = 14.8 Hz, ^3J = 6.0 Hz, *A*BX), 5.49 (bd, 1H, ^3J = 8.5 Hz, AB*X*), 6.19 (bs, 1H), 7.20-7.36 (m, 5H); ^{13}C NMR (90 MHz, $CDCl_3$) δ 18.4, 28.4, 29.4, 43.6, 46.3, 46.6, 79.4, 127.5, 127.7, 128.7, 138.3, 155.3, 173.0; HRMS (ESI+) Calcd for $C_{17}H_{24}N_2NaO_3$ $[M + Na]^+$: 327.1679, found 327.1673.

X-ray structures

Crystal data has been deposited to the Cambridge Crystallographic Database with CCDC number 1908274 (Boc−(c-ACBC)−NH−CB) and contain the supplementary crystallographic data for this paper. These data can be obtained free of charge from The Cambridge Crystallographic Data Centre via www.ccdc.cam.ac.uk/data_request/cif.[26]

EXPERIMENTAL SPECTROSCOPIC METHODS

The vibrational IR absorption and VCD spectra were measured using an FTIR spectrometer (Vertex 70, Bruker) equipped with a VCD module (PMA 50, Bruker). The signal was measured by an MCT IR detector equipped with a BaF_2 window and cooled with liquid nitrogen. A spectral resolution of 4 cm^{-1} was used for both absorption and VCD spectra. The IR radiation was polarized with a linear polarizer then modulated by a 50 kHz ZnSe photo-elastic modulator (Hinds). A low-pass filter cutting at 2000 cm^{-1} was added before the linear polarizer to increase the dynamical response of the detector. The signal of the MCT detector was demodulated using a lock-in amplifier (Stanford Research Systems SR 830). The alignment of the spectrometer was carefully verified by checking the mirror-image relation between the VCD spectra of the two enantiomers of camphor (0.3 M in CCl_4). The samples were prepared by grinding 6 mg of the studied molecule with 2 g of KBr in a mixer mill (MM 400 Retsch) at 20 Hz during 1 h. The artefacts due to the birefringence of the KBr pellets were eliminated by following the procedure proposed by Merten,[27] derived from that introduced by Buffeteau.[28] It consists in rotating the sample in the plane perpendicular to the light propagation axis for each side (front F or back B) of the pellet and averaging the spectra obtained for each position of the pellet at 0° and 90° (Equation 1).

$$I^{VCD}(\tilde{\nu}) = \frac{1}{8}\sum_{n=0}^{3} I^{VCD}(\tilde{\nu}; n\cdot 90°; F) + I^{VCD}(\tilde{\nu}; n\cdot 90°; B) \qquad (1)$$

For the sake of better averaging and artefact control, the procedure was extended to 180° and 270°. The measurements were repeated on a second sample. The final spectrum was obtained by adding 1400 scans for each sample position and averaging all the positions so that the total acquisition time is ~5 h 30 for all the spectra shown below.

THEORETICAL METHODS

The calculation strategy encompassed the following steps, which rest on the X-ray structures. Single crystal X-ray diffraction data for *cis*-ACBC and *trans*-ACBC were not available for this study; instead, we used the X-ray data of the related compounds *cis*-ACBC* and *trans*-ACBC*, in which the benzyl amide (Bn) is replaced by a cyclobutyl amide (*c*-Bu), shown in Figure 1. Firstly, a supramolecular unit of the molecule under study was constructed from the crystal of the model structure. The hydrogen bond pattern was kept identical to that of the model system and the cyclobutyl is substituted by a benzyl. The preliminary structure obtained thereby was optimized using periodic boundary conditions (PBC). The PBC calculations were limited to one-dimension along the b axis, *i.e.* the hydrogen bonded strands. Then a core of finite size was extracted from the resulting structure. The IR absorption and VCD spectra were calculated for increasing sizes of the core until the calculations satisfactorily reproduce the experimental results, which allows determining the smallest cluster size that is necessary for reproducing the VCD spectrum of the crystal. The RI B97-D/TZVPP –D3 calculations were performed using the Turbomole package.[29] All the other calculations were performed using the Gaussian 09 program.[30]

Optimization of the preliminary structure using PBC was performed at the B3LYP/6-31G level of theory, with sixteen units per cell. A core of four molecules was then extracted from the PBC results and calculated at the RI B97-D/TZVPP –D3 level which is known to yield satisfactory frequencies for peptides at an acceptable computational cost. For the sake of testing the ability of simpler assembly to account for the experimental data, dimers and monomers were also extracted from this tetramer. The resolution of the identity was used for reducing the calculation time.[31] The harmonic frequencies were calculated at the same level of theory. Dispersion-corrected calculations, with the same basis set and functional, were used previously for the same molecules isolated in the gas phase and yielded excellent agreement with the experimental values.[8] The calculated harmonic frequencies were scaled in the 3 μm region to correct them for anharmonicity and basis set incompleteness. The scaling factor used (0.96) was defined as the ratio between the experimental frequencies of the conformers observed in the gas phase and the harmonic frequencies calculated at the RI B97-D/TZVPP level. This value is found to be insensitive to the fact that dispersion corrections are used or not. No scaling factor was needed in the fingerprint region.

Then, the VCD spectra were calculated for increasing sizes of clusters extracted from the tetramer, stopping at the smallest size that gives satisfactory agreement with the experiment. VCD calculations were carried out, with the previously obtained geometries, at the B3LYP/6-31G++(d,p) level for the monomers and 6-31G(d,p) level for the dimers or the tetramers.[32] The 6-31G++(d,p) level was chosen because it has been shown to give satisfactory results in calculating VCD spectra of flexible molecules.[33] Moreover, using the smaller basis set 6-31G(d,p) gives results similar to those at the B3LYP/6-31G++(d,p) level for cyclic dipeptides and allows calculating large systems at a reasonable computational cost.[15c] Here also, similar results are

obtained with the two levels of theory, as shown in Figure S1 on the example of the **Mcis** *cis*-ACBC monomer, extracted from the tetramer, and eventually used for the assignment (*vide infra*). In order to test the sensitivity of the VCD signals to dispersion interactions as will be discussed below, calculations have been carried out in the presence or absence of the D3 set of dispersion parameters.[34] When not specified otherwise, the reported calculations do not include dispersion. All the monomers observed in the gas phase and reported previously were recalculated here, including dispersion or not, for the sake of comparison. The harmonic frequencies were scaled by 0.96 in the 3 μm region, *i.e.* the ratio between the experimental frequencies in the gas phase and the harmonic calculated frequencies, and 0.97 in the fingerprint region.

Results and Discussion

CRYSTALLOGRAPHIC DATA

The crystal structure of model systems *cis*-ACBC* and *trans*-ACBC*is shown in Figure 2. Both *cis*-ACBC* and *trans*-ACBC* compounds show infinite strands of monomers bound by intermolecular NH···OC hydrogen bonds. The chains observed for the *cis* derivative involve head-to-head alignment of the monomeric subunits, which results to antiparallel NH···OC hydrogen bonds. Two sorts of hydrogen bonds are therefore expected to be spectroscopically observed, namely, $N_4H\cdots OC_3$ and $N_{10}H\cdots OC_9$. The crystal structure of the *trans* derivative shows a head-to-tail arrangement of the sub-units with parallel NH···OC hydrogen bonds. The parallel double hydrogen bond involves $N_4H\cdots OC_9$ and $N_{10}H\cdots OC_3$ hydrogen bonds. If we assume a similar crystal structure for the model systems and the compounds studied here, all the phenyl rings are on the same side of the strand in the *cis* derivative. We can anticipate that this arrangement has consequences in terms of dispersion energy and packing effect. Conversely, the aromatic substituents are on alternating sides in the *trans* compound. The hydrogen bond distances and important structural parameters of the model systems are listed in Tables 1 and 2.

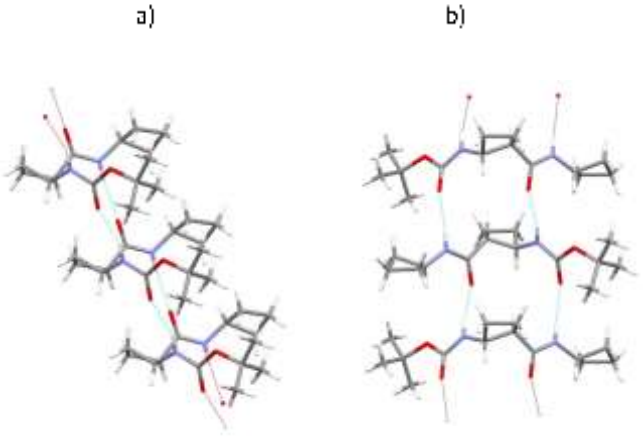

FIGURE 2 Crystallographic structure of a) *cis*-ACBC* and b) *trans*-ACBC* showing the head-to-head and head-to-tail arrangement of the molecules.

GAS-PHASE SPECTROSCOPIC DATA$

cis-ACBC and *trans*-ACBC have been fully characterised in the gas phase by conformer-selective laser spectroscopy under supersonic expansion conditions.[8] In brief, the experimentally observed conformation of *trans*-ACBC has been assigned to a structure involving an 8-member ring (C8) bridging the N(10)H and C(3)O groups, named **t-1**. The C8 interaction is outstandingly strong and manifests itself by a broad red shifted feature at 3021 cm^{-1} assigned to the ν(NH) stretch. It should be noted that the most stable calculated structure **t-1** involves interaction between the *t*-butyl group and the phenyl ring, a point to which we shall return in the discussion.[8] Two conformers have been experimentally observed for *cis*-ACBC. The most intense bands of the electronic spectrum have been assigned to a C8 structure, named **c-1**, while weaker electronic transitions have been attributed to a C6 structure, named **c-3**. Due to the close position of the two amide functions, only frustrated hydrogen bonds can be formed. As a result, the C8 interaction is much weaker in *cis*-ACBC than in *trans*-ACBC, with a ν(NH) stretch observed at 3414 cm^{-1}, compared to the free ν(NH) stretch observed at 3485 cm^{-1}. The C6 structure displays a weak C6 hydrogen bond, with bounded and free ν(NH) stretches observed at 3465 and 3480 cm^{-1}, respectively. Interestingly, a second conformer of the C8 form of both *cis* and *trans*-ACBC, namely **t-2** or **c-2**, was calculated, with similar ΔG at room temperature as **t-1** or **c-1**, with similar H-bonding pattern but no interaction between the phenyl and *t*-butyl groups. It was supposed that this second conformer relaxes to the most stable one in the late expansion. It should be noted however that due to the similar hydrogen bond patterns of **t-2** and **t-1**, and of **c-1** and **c-2**, respectively, these forms could not be distinguished based on their IR spectra only.

SOLID-PHASE SPECTROSCOPIC RESULTS

cis-ACBC

The experimental IR absorption and VCD spectra of *cis*-ACBC in the fingerprint region are shown in Figures 3a and 3c, respectively. The comparison between the VCD spectra of the two enantiomers is given in Figure S2. The IR absorption shows two bands in the Amide I region (ν(CO) stretches), located at 1681 and 1650 cm^{-1}. These bands appear as singlets of identical sign in the VCD spectra. The shape of the spectrum, in particular, an identical sign for the two ν(CO) stretches, suggests a structure in which the ν(CO) stretches are not coupled.

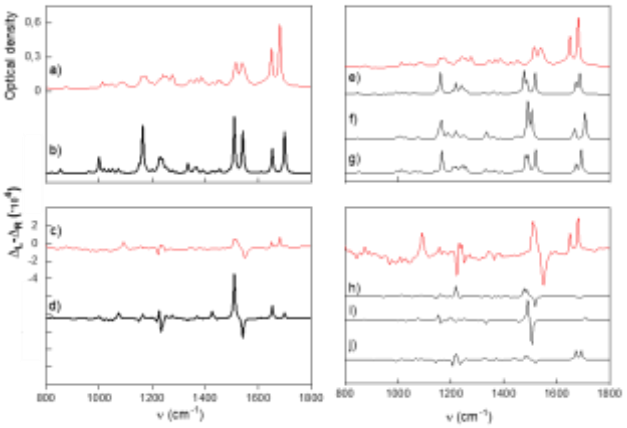

FIGURE 3 Left: a) Experimental IR absorption of *cis*-ACBC (1*R*,2*S*) (red) b) calculated IR absorption of the monomer subunit **Mcis** c) Experimental VCD spectrum of (1*R*,2*S*) (red) d) calculated VCD spectrum of the monomer subunit (see text). Right: Experimental IR absorption of *cis*-ACBC (1*R*,2*S*) (red) and calculated IR absorption of e) **c-1** f) **c-3** g) **c-2**. e) Experimental VCD spectra of *cis*-ACBC (1*R*,2*S*) (red) and calculated VCD spectrum of h) **c-1** i) **c-3** j) **c-2**. The calculations are at the B3LYP /6-31G++(d, p) level. The harmonic frequencies are scaled by 0.97.

The Amide II region (β(NH) bends) displays two broader bands, at 1537 cm^{-1} and 1520 cm^{-1}, which appear as a bisignate doublet in the VCD spectrum. The presence of a doublet may indicate either coupled modes or two non-coupled vibrations with opposite rotatory strengths.[15c] The intensity (difference in absorbance between left and right circular polarised light) of the bands is of the order of 10^{-4} for the strongest features. The spectrum of a tetramer core calculated at the RI B97-D/TZVPP level including or not D3 corrections is compared to the experiment in Figures S3. In both cases, the hydrogen-bonded strand tends to bend when the chain length increases, which results in non-equivalent hydrogen bonds. Calculations including dispersion tend to deform the structure more than those that do not include dispersion, which results in a less satisfactory agreement between experimental and simulated spectra, probably because the interaction with the adjacent strands is not taken into account. However, the hydrogen bond pattern in the core of the oligomer is similar whatever the method used. We have therefore extracted a monomer from this core, referred to as **Mcis** hereafter. Figure 3b and 3d show the calculated IR absorption and the VCD spectra calculated at the B3LYP level for **Mcis**. It should be noted here that optimising **Mcis** with dispersion correction results to the folding of the molecule and a wrong VCD signature in the region of the ν(CO) stretch. For this reason, we have performed the calculations at the B3LYP/6-31G++(d,p) level with no dispersion corrections. The calculations with dispersion corrections are shown in Figure S4 of the supplementary information. The spectrum of the monomers present in the gas phase, namely **c-1** and **c-3**, as well as that of **c-2**, are shown in Figure 3f, 3g, 3h, respectively, for the sake of comparison. These three structures are shown in Figure 4. The IR absorption spectrum of the most stable gas-phase structures qualitatively agrees with the experimental IR absorption spectrum but better agreement is obtained between the experiment and the spectra of **Mcis**. In particular, the spacing between the CO stretch frequencies is well reproduced in the simulated IR absorption spectrum of **Mcis**. The CO···HN distances of this monomeric subunit are intermediate between that of the so-called **c-1** and **c-3** structures evidenced in the gas phase (see Table 1). Indeed, the N4H···OC9 and N10H···OC3 distances are 3.37 and 3.84 Å, respectively. Still, **Mcis** resembles **c-3** more than **c-1**, which explains that the agreement between experiment and calculated IR absorption spectra is slightly better for **c-3** than **c-1**. **Mcis** displays a completely extended structure, with ψ_{Ph} = -83°. The distance between O2 and H13 is large (10.49 Å), compared to 5.74 and 8.38 Å for **c-1** and **c-3**, respectively. This extended geometry allows interaction between the benzene substituents of two neighbouring molecules. It is reminiscent of the calculated **c-2** geometry, in which this distance is 9.76 Å.

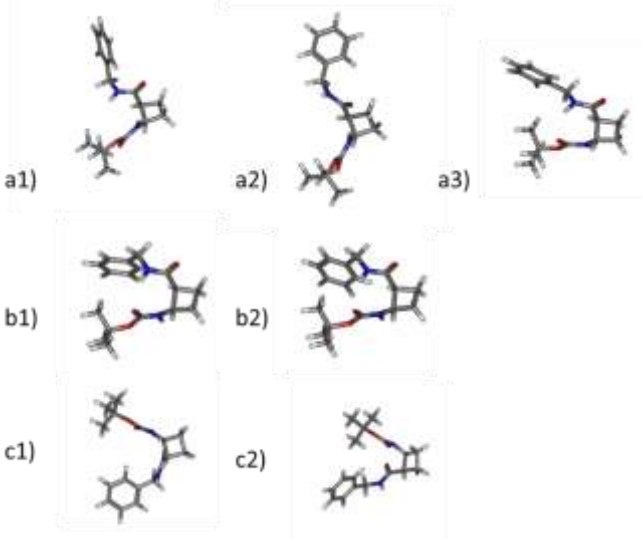

FIGURE 4 Structures of *cis*-ACBC (1*R*,2*S*) calculated at the B3LYP-D3/6-31G++(d,p) level of theory. a1) **Mcis** monomer as it is in the supramolecular structure (see text) a2) **Mcis** monomer optimised without dispersion a3) **Mcis** monomer optimised with dispersion b1) c1 structure evidenced in the gas phase, with a C8 intramolecular hydrogen bond, optimised without dispersion b2) same with dispersion c) c3 structure evidenced in the gas phase, with a C6 intramolecular hydrogen bond optimised without dispersion, c2) same with dispersion.

The experimental VCD spectrum, shown in Figure 3c, can be divided into two regions. The amide II region where the observed bisignate signature is satisfactorily reproduced by any of the structures mentioned above. It is neither sensitive to the nature of the intramolecular H bond nor to the position of the substituents. The bisignate doublet corresponds to the β(N4H) and β(N10H) bends, which display opposite VCD signs. The lack of sensitivity of the VCD signal of these modes to the environment and structural parameters is characteristic of what are called robust modes.[14, 35 36] Indeed, **c-1**, **c-3**, **c-2**, and **Mcis** show a similar bisignate pattern in this range, except for slight differences in intensities. Depending on the structure considered, the two β(NH) bends are coupled (in **c-3**) or not (in **Mcis**) but the shape of the VCD spectrum in this range remains similar, with two bands of opposite signs. Also, examination of the structures shown in Figure 4 indicates that the relative position of the NH is not the same in the three systems. In **c-1**, the two NH make an angle of ~30°, while this angle is only of the order of ~5° in **Mcis** and close to zero in **c-3**. Including dispersion in the calculation or not does not alter the shape of the spectrum either.

The ν(CO) stretch region displays much more variability. In **c-1**, the ν(CO) stretches are slightly coupled and a band of the wrong sign is calculated. In **c-3** or **Mcis**, the ν(CO) stretches are completely localized and appear as signals of identical sign. In order to check whether the localized or delocalized character of the ν(CO) stretches really is what impinges the shape of the VCD spectrum, we have compared the calculated spectrum of **c-1**, which is the most stable conformer in the gas phase, to that of **c-2**. **c-2** displays exactly the same hydrogen bond pattern as **c-1** but differs in the position of the phenyl, which is interacting with the BOC substituent in **c-1** but not in **c-2**. The IR absorption spectra of **c-1** and **c-2** are identical, as shown in Figure 3. The bisignate signature observed in the region of the β(NH) stretches is similar in **c-2** and **c-1**, although slightly more intense in **c-1**. The two

conformers completely differ in the shape of their VCD spectrum in the region of the ν(CO) stretches. While **c-1** displays a single band of the wrong sign, **c-2** shows two bands of identical sign, as experimentally observed. The ν(CO) stretching modes are slightly coupled in **c-2**, like in **c-1**, but their VCD signatures in the ν(CO) stretch region are different.

We can also examine the effect of including dispersion. For a given geometry, including dispersion in the frequency calculations does not modify the IR and VCD spectra. However, at the geometry optimization stage, dispersion tends to make the *t*-butyl and aromatic ring closer to each other, which in turn results in shorter NH…OC distances. As a result, the ν(CO) stretching modes, which are only slightly coupled in **c-1** optimised without dispersion corrections, are fully delocalised when **c-1** is optimised including D3 corrections. This change is also reflected in the shape of the VCD spectrum in the ν(CO) stretch region (see Figure S4). Dispersion also modifies the VCD spectrum of **c-3**. When optimization is performed without dispersion, **c-3** shows two bands of identical sign, but the low-energy one is so weak that it cannot be distinguished in the spectrum. When including dispersion in the calculations, two bands of comparable intensity are observed. This example illustrates the extreme sensitivity of VCD to subtle structural parameters, in this case, dispersion driven structural modifications. When including dispersion, the optimisation of **Mcis** results in a structure similar to **c-1**, hence an unsatisfactory VCD spectrum. We can conclude from these results that the presence of two bands of identical sign in the ν(CO) stretch region is the signature of an open structure, and can be taken as an indication of non-interacting *t*-butyl and phenyl ring. We can also conclude that description of dispersion is of extreme importance here as overestimating dispersion results in a folded geometry and hence in wrong VCD spectrum in the ν(CO) stretch region.

***trans*-ACBC**

The IR absorption and the VCD spectra of *trans*-ACBC in the fingerprint region are shown in Figures 5a and 5e. The comparison between the VCD spectra of the two enantiomers is given in Figure S5. Only one absorption band appears in the β(NH) region, at 1535 cm^{-1}, a value characteristic of a bound NH group. This band is broader (18 cm^{-1} FWMH) than the other features observed in the IR absorption spectrum and probably corresponds to the superposition of β(NH) bending modes of different nature but similar frequencies. In contrast, two bands are observed in the ν(CO) stretch region, in ranges characteristic of the ν(C3O) (ester) (1684 cm^{-1}) and ν(C9O) (amide) (1645 cm^{-1}) stretches. Each ν(CO) and β(NH) band observed in absorption appears as a bisignate couplet in the VCD spectrum. The VCD spectrum is much more intense than that of *cis*-ACBC, with the strongest intensity, of the order of 10^{-3}, being one order of magnitude larger than in *cis*-ACBC. However, the intensity in the β(NH) range is of the same order as in *cis*-ACBC, the major difference is observed in the ν(CO) range.

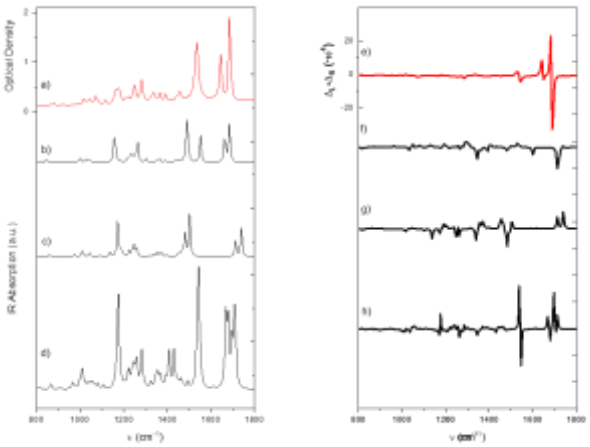

FIGURE 5 a) Experimental IR absorption of (1*S*,2*S*) *trans*-ACBC (red). Calculated IR absorption of b) the monomer **t-1** in the gas phase c) the monomer **Mtrans** (see text) d) the tetramer subunit. e) Experimental VCD spectrum of *trans*-ACBC (1*S*,2*S*) (red). Calculated VCD spectrum of f) the monomer **t-1** in the gas phase g) the monomer **Mtrans** (see text) h) the tetramer subunit. In the tetramer; the two NH and CO of the termini have been isotopically modified by tritium and O18, respectively, to minimize boundary effects. The calculations are at the B3LYP/6-31G ++(d, p) level. The frequencies are scaled by 0.97.

We have followed the same procedure as for *cis*-ACBC and optimised the tetramer extracted from the PBC calculations at the B97-D3 level. As observed for *cis*-ACBC, including dispersion results to a folding of the hydrogen-bonded strand, hence poorer agreement between experimental and simulated IR spectra. Thus, we have favoured calculations without dispersion corrections. The simulated IR absorption deduced from calculations without dispersion corrections is compared to the experiment in Figure S6. Notwithstanding the boundary effects, the IR absorption spectra show satisfactory agreement with the experiment, in particular, the gap between the β(NH) and the ν(CO) is correctly reproduced.

The monomer extracted from the PBC calculations, called **Mtrans** in what follows, qualitatively reproduces the observed IR absorption, in contrast with the gas-phase most stable monomer **t-1** for which the bound β(NH) is calculated much too high in energy relative to the experiment (see Figure 5). This suggests that the intramolecular C8 hydrogen bond observed in the gas phase is disrupted in the solid to the benefit of intermolecular hydrogen bonds. These intramolecular hydrogen bonds are not as strong as the intramolecular C8 interaction evidenced in the gas phase monomer. The spacing between the β(NH) bend and the ν(CO) stretch frequencies calculated in **Mtrans** is overestimated relative to the experiment. Moreover, there is no mean of describing the VCD spectrum in terms of a monomer only. Indeed, the fact that each absorption band appears as a bisignate doublet indicates that a cluster must be considered. However, the dimer does not reproduce the IR spectrum, in particular, the gap between the β(NH) bend and the ν(CO) stretch bands (see Figure S5). Moreover, the two ν(CO) stretch transitions appear in the region of bound ν(CO) and show a bisignate signature. This suggests that a structure with at least four bonded COs, *i.e.* a tetramer, should be taken into account. We therefore calculated the IR absorption and the VCD spectra of the tetramer, at the B3LYP/6-31G(d,p) level. To avoid consequences of boundary effects in the vibrational spectroscopy, the termini were

isotopically modified. The hydrogen atoms of the two free NH were replaced by tritium and the oxygen atoms of the two free CO by the ^{18}O isotope. The resulting structure, shown in Figure 6, shows the typical OH···N double strand zigzag pattern. The intermolecular hydrogen bonds are slightly longer (d(O3···NH10) = 1.94 Å) between the amide NH and the ester CO than between the ester NH and the amide CO (d(O9···NH4 = 1.91 Å), as it is the case for *trans*-ACBC* (see Table 2). The ψ_{Ph} angle (99°) is typical of an open structure, which allows interaction between two neighbouring molecules, as it was already described for *cis*-ACBC. The phenyl rings are indeed involved in an interaction with the neighbouring molecule that involves a CH group of the ACBC ring (C6H···π interaction). The tetramer satisfactorily reproduces the IR absorption, as shown in Figure 5. The VCD signature is well reproduced in the region of the β(NH) bend as this region shows two bands of opposite sign. The ν(CO) stretch region also shows bisignate signatures, although the intensity enhancement is not reproduced in the calculations. Still, the gap between the β(NH) bend and the ν(CO) stretch transitions is still slightly overestimated relative to the experiment. Moreover, the ratio between the ν(NH) intensity to that of the ν(CH) is still underestimated in the calculated spectrum of the tetramer relative to the experiment. This suggests that chains larger than four units should be taken into account.

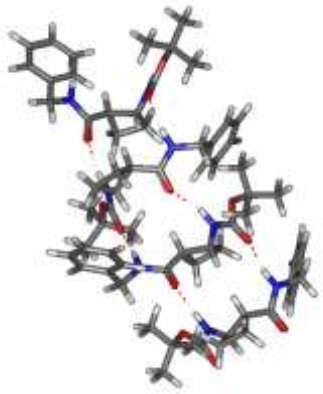

FIGURE 6 Calculated structure of the *trans*-ACBC tetramer calculated at the B3LYP/6-31G(d,p) level of theory. Dashed lines indicate the hydrogen bonds.

DISCUSSION: LOCALISED *vs.* DELOCALISED VIBRATIONAL MODES

The main difference experimentally observed between *cis* and *trans*-ACBC compounds appear in the region of the ν(CO) stretching modes. While the VCD signature in the β(NH) range is similar in shape and intensity for *cis* and *trans*-ACBC, the VCD intensity of the ν(CO) bands is one order of magnitude larger in the *trans* compounds. It should be noted that the intensity enhancement is also observed for the IR absorption in the region of the ν(NH) stretch. This is however not reproduced in the calculation as already described by Marty et *al.* in their description of VCD enhancement in perylene bisimide oligopeptides.[18] A very recent calculation of the VCD signal of solid alanine by means of *ab initio* molecular dynamics (AIMD) and nuclear velocity perturbation theory (NVPT) has explained the enhancement of the VCD signal in terms of supramolecular helical arrangement of the oscillators.[23] One of the important conclusions of the latter work is that the intense VCD signal of the carbonyl bands is exclusively explained in terms of supramolecular effects and that considering coupled oscillator on a minimum intermolecular distance of 4-5 Å is necessary for reproducing the experimentally observed enhancement. We can raise the question as to whether such supramolecular effects also play a role to explain the spectroscopic properties of *trans*-ACBC. To test this hypothesis, we have calculated a subunit of two parallel hydrogen-bonded dimers, in a geometry similar to that of two parallel strands in the crystal. However, the IR absorption of this sub-unit (not shown) is completely at odds with the experimental spectrum. These results point at a long-range organisation of the solid, along the axis of the hydrogen bonds as the main feature responsible for the observed spectral gap between ν(CO) and β(NH) bands. Still, the coupling between two parallel strands could be responsible for intensity enhancement in the VCD spectrum of *trans*-ACBC. However, it is not clear why this effect would play a determining role in *trans*-ACBC or alanine, and not in *cis*-ACBC, although alanine and the two model systems for *cis* and *trans*-ACBC the three molecules have the same space group $P2_12_12_1$. The size of the systems studied here precludes the use of AIMD methods, but polarizable force fields would be interesting for calculating the VCD spectra of such complex molecules in a solid environment.[37]

Conclusion

We have studied the IR absorption and VCD spectra of Boc−(*cis*-ACBC)−NH−Bn and Boc−(*trans*-ACBC)−NH−Bn. In *cis*-ACBC, the fact that the VCD spectrum is well reproduced by considering the monomer as the smallest unit in the solid indicates that long-distance intermolecular couplings can be neglected. The intensity of the VCD signal of *trans*-ACBC is one order of magnitude larger than that of *cis*-ACBC in the region of the ν(CO) stretch. The two intense bisignate couplets observed for the ν(CO) stretching modes are qualitatively reproduced by a one-dimension tetramer involving the head-to-tail arrangement of the sub-units with parallel NH···OC hydrogen bonds. Calculations on smaller model systems indicate that the gap between the ν(CO) stretch and the β(NH) bend decreases when the chain length increases and that although the calculations have been limited to four units, including six units improves this gap and shows extensive delocalisation of the ν(CO) stretches in a “zigzag” fashion. The inclusion of parallel strands might be necessary for reproducing the intensity of the bisignate VCD couplets observed for the ν(CO) stretches but are out of reach due to the size of the systems.

Acknowledgements

Support from the French National Research Agency (ANR) is acknowledged (Grant ANR-11-IDEX-0003-02 and ANR-17-CE29-0008).We thank Antoine Béthune for his experimental contribution. We acknowledge the use of the computing facility cluster MésoLUM of the LUMAT federation (FR LUMAT 2764).

Supporting information

Additional supporting information may be found in the online version of this article at the publisher’s website.

REFERENCES AND NOTES

12. Disney MD, Hook DF, Namoto K, Seeberger PH and Seebach D, *Chemistry & Biodiversity* **2005**, *2*, 1624-1634.
17. Szolnoki E, Hetenyi A, Mandity IM, Fulop F and Martinek TA, *European Journal of Organic Chemistry* **2013**, 3555-3559.
17. Choi SH, Ivancic M, Guzei IA and Gellman SH, *European Journal of Organic Chemistry* **2013**, 3464-3469.
37. Grison CM, Miles JA, Robin S, Wilson AJ and Aitken DJ, *Angewandte Chemie-International Edition* **2016**, *55*, 11096-11100.
11. Torres E, Gorrea E, Da Silva E, Nolis P, Branchadell V and Ortuno RM, *Organic Letters* **2009**, *11*, 2301-2304.
3. Torres E, Gorrea E, Burusco KK, Da Silva E, Nolis P, Rua F, Boussert S, Diez-Perez I, Dannenberg S, Izquierdo S, Giralt E, Jaime C, Branchadell V and Ortuno RM, *Organic & Biomolecular Chemistry* **2010**, *8*, 564-575.
4. Pohl G, Gorrea E, Branchadell V, Ortuno RM, Perczel A and Tarczay G, *Amino Acids* **2013**, *45*, 957-973.
46. Alauddin M, Gloaguen E, Brenner V, Tardivel B, Mons M, Zehnacker-Rentien A, Declerck V and Aitken DJ, *Chemistry-a European Journal* **2015**, *21*, 16479-16493.
16. Fernandes C, Faure S, Pereira E, Théry V, Declerck V, Guillot R and Aitken DJ, *Organic Letters* **2010**, *12*, 3606-3609.
20. Izquierdo S, Rua F, Sbai A, Parella T, Alvarez-Larena A, Branchadell V and Ortuno RM, *Journal of Organic Chemistry* **2005**, *70*, 7963-7971.
41. Gobi S, Knapp K, Vass E, Majer Z, Magyarfalvi G, Hollosi M and Tarczay G, *Physical Chemistry Chemical Physics* **2010**, *12*, 13603-13615.
48. Kubelka J and Keiderling TA, *Journal of the American Chemical Society* **2001**, *123*, 12048-12058; 5. Keiderling TA, *Current Opinion in Chemical Biology* **2002**, *6*, 682-688; 1. Toniolo C, Formaggio F, Tognon S, Broxterman QB, Kaptein B, Huang R, Setnicka V, Keiderling TA, McColl IH, Hecht L and Barron LD, *Biopolymers* **2004**, *75*, 32-45; 1-3. Kim J, Kapitan J, Lakhani A, Bour P and Keiderling TA, *Theoretical Chemistry Accounts* **2008**, *119*, 81-97; 15. Lee KK, Oh KI, Lee H, Joo C, Han H and Cho M, *Chemphyschem* **2007**, *8*, 2218-2226; 22. Beke T, Somlai C, Magyarfalvi G, Perczel A and Tarczay G, *Journal of Physical Chemistry B* **2009**, *113*, 7918-7926.
8. Huang R, Kubelka J, Barber-Armstrong W, Silva R, Decatur SM and Keiderling TA, *Journal of the American Chemical Society* **2004**, *126*, 2346-2354; 4. Moretto A, Crisma M, Formaggio F, Toniolo C, Wu L, Keiderling TA, Kaptein B and Broxterman QB, *Biopolymers* **2007**, *88*, 556-556; 24. Kessler J, Keiderling TA and Bour P, *Journal of Physical Chemistry B* **2014**, *118*, 6937-6945.
9. Gobi S, Magyarfalvi G and Tarczay G, *Chirality* **2015**, *27*, 625-634.
1. Kubelka J, Kim J, Bour P and Keiderling TA, *Vibrational Spectroscopy* **2006**, *42*, 63-73; 1. Prusa J and Bour P, *Chirality* **2018**, *30*, 55-64; 2. Perez-Mellor A and Zehnacker A, *Chirality* **2017**, *29*, 89-96.
5. Hassoun A, Grison CM, Guillot R, Boddaert T and Aitken DJ, *New Journal of Chemistry* **2015**, *39*, 3270-3279; 4. Celis S, Gorrea E, Nolis P, Illa O and Ortuno RM, *Organic & Biomolecular Chemistry* **2012**, *10*, 861-868.
12. Jiang N, Tan RX and Ma J, *Journal of Physical Chemistry B* **2011**, *115*, 2801-2813.
38. Marty R, Frauenrath H and Helbing J, *Journal of Physical Chemistry B* **2014**, *118*, 11152-11160.
43. Frelek J, Gorecki M, Laszcz M, Suszczynska A, Vass E and Szczepek WJ, *Chemical Communications* **2012**, *48*, 5295-5297.
1. Castellucci N, Falini G, Milli L, Monari M, Abbate S, Longhi G, Castiglioni E, Mazzeo G and Tomasini C, *Chempluschem* **2014**, *79*, 114-121.
25. Buffeteau T, Ducasse L, Poniman L, Delsuc N and Huc I, *Chemical Communications* **2006**, 2714-2716; 1. Moreno JRA, Urena FP and Gonzalez JJL, *Structural Chemistry* **2011**, *22*, 67-76.
30. Quesada-Moreno MM, Cruz-Cabeza AJ, Aviles-Moreno JR, Cabildo P, Claramunt RM, Alkorta I, Elguero J, Zuniga FJ and Lopez-Gonzalez JJ, *Journal of Physical Chemistry A* **2017**, *121*, 5665-5674.
40. Jahnigen S, Scherrer A, Vuilleumier R and Sebastiani D, *Angewandte Chemie-International Edition* **2018**, *57*, 13344-13348.
18. Rode JE, Lyczko K, Jawiczuk M, Kawecki R, Stanczyk W, Jaglinska A and Dobrowolski JC, *Chemphyschem* **2018**, *19*, 2411-2422.
Declerck V and Aitken DJ, *Amino Acids* **2011**, *41*, 587.
Altmayer-Henzien A, Declerck V, Guillot R and Aitken DJ in *Experimental Crystal Structure Determination CCDC 888820*, *Vol.* **2016**.
8. Merten C, Kowalik T and Hartwig A, *Applied Spectroscopy* **2008**, *62*, 901-905.
6. Buffeteau T, Lagugne-Labarthet FS and Sourisseau C, *Applied Spectroscopy* **2005**, *59*, 732-745.
3. Ahlrichs R, Bar M, Haser M, Horn H and Kolmel C, *Chemical Physics Letters* **1989**, *162*, 165-169.
M. J. Frisch GWT, H. B. Schlegel, G. E. Scuseria, M. A. Robb, J. R. Cheeseman, G. Scalmani, V. Barone, B. Mennucci, G. A. Petersson, H. Nakatsuji, M. Caricato, X. Li, H. P. Hratchian, A. F. Izmaylov, J. Bloino, G. Zheng, J. L. Sonnenberg, M. Hada, M. Ehara, K. Toyota, R. Fukuda, J. Hasegawa, M. Ishida, T. Nakajima, Y. Honda, O. Kitao, H. Nakai, T. Vreven, J. A. Montgomery, J. E. Peralta, F. Ogliaro, M. Bearpark, J. J. Heyd, E. Brothers, K. N. Kudin, V. N. Staroverov, R. Kobayashi, J. Normand, K. Raghavachari, A. Rendell, J. C. Burant, S. S. Iyengar, J. Tomasi, M. Cossi, N. Rega, J. M. Millam, M. Klene, J. E. Knox, J. B. Cross, V. Bakken, C. Adamo, J. Jaramillo, R. Gomperts, R. E. Stratmann, O. Yazyev, A. J. Austin, R. Cammi, C. Pomelli, J. W. Ochterski, R. L. Martin, K. Morokuma, V. G. Zakrzewski, G. A. Voth, P. Salvador, J. J. Dannenberg, S. Dapprich, A. D. Daniels, Farkas, J. B. Foresman, J. V. Ortiz, J. Cioslowski, D. J. Fox, **2010**.
1-4. Weigend F and Haser M, *Theoretical Chemistry Accounts* **1997**, *97*, 331-340.
Halls MD, Velkovski J and Schlegel HB, *Theoretical Chemistry Accounts* **2001**, *105*, 413; 15. Grimme S, Antony J, Ehrlich S and Krieg H, *Journal of Chemical Physics* **2010**, *132*; 7. Grimme S, Ehrlich S and Goerigk L, *Journal of Computational Chemistry* **2011**, *32*, 1456-1465.
21. Le Barbu-Debus K, Scherrer A, Bouchet A, Sebastiani D, Vuilleumier R and Zehnacker A, *Physical chemistry chemical physics : PCCP* **2018**, *20*, 14635-14646.
14. Goerigk L and Grimme S, *Physical Chemistry Chemical Physics* **2011**, *13*, 6670-6688.
Nicu VP and Baerends EJ, *Physical Chemistry Chemical Physics* **2009**.
24. De Gussem E, Bultinck P, Feledziak M, Marchand-Brynaert J, Stevens CV and Herrebout W, *Physical Chemistry Chemical Physics* **2012**, *14*, 8562-8571.
8. Ponder JW, Wu CJ, Ren PY, Pande VS, Chodera JD, Schnieders MJ, Haque I, Mobley DL, Lambrecht DS, DiStasio RA, Head-Gordon M, Clark GNI, Johnson ME and Head-Gordon T, *Journal of Physical Chemistry B* **2010**, *114*, 2549-2564; Thaunay F, Dognon JP, Ohanessian G and Clavaguéra C, *Phys. Chem. Chem. Phys.* **2015**, *17*, 25968-25977.

Graphical Abstract